Plasticity in Amorphous Solids Is Mediated by Topological Defects in the Displacement Field

Matteo Baggioli,[1,2,†] Ivan Kriuchevskyi,[3,‡] Timothy W. Sirk,[4,§] and Alessio Zaccone[3,5,*]
[1]*Wilczek Quantum Center, School of Physics and Astronomy, Shanghai Jiao Tong University, Shanghai 200240, China*
[2]*Shanghai Research Center for Quantum Sciences, Shanghai 201315, China*
[3]*Department of Physics "A. Pontremoli," University of Milan, via Celoria 16, 20133 Milan, Italy*
[4]*Polymers Branch, U.S. Army Research Laboratory, Aberdeen Proving Ground, Maryland 21005, USA*
[5]*Cavendish Laboratory, University of Cambridge, J J Thomson Avenue, CB30HE Cambridge, United Kingdom*

(Received 15 January 2021; revised 31 March 2021; accepted 25 May 2021; published 2 July 2021)

The microscopic mechanism by which amorphous solids yield plastically under an externally applied stress or deformation has remained elusive in spite of enormous research activity in recent years. Most approaches have attempted to identify atomic-scale structural "defects" or spatiotemporal correlations in the undeformed glass that may trigger plastic instability. In contrast, in this Letter we show that the topological defects that correlate with plastic instability can be identified, not in the static structure of the glass, but rather in the nonaffine displacement field under deformation. These dislocation-like topological defects (DTDs) can be quantitatively characterized in terms of Burgers circuits (and the resulting Burgers vectors) that are constructed on the microscopic nonaffine displacement field. We demonstrate that (i) DTDs are the manifestation of incompatibility of deformation in glasses as a result of violation of Cauchy-Born rules (nonaffinity); (ii) the resulting average Burgers vector displays peaks in correspondence of major plastic events, including a spectacular nonlocal peak at the yielding transition, which results from self-organization into shear bands due to the attractive interaction between antiparallel DTDs; and (iii) application of Schmid's law to the DTDs leads to prediction of shear bands at 45° for uniaxial deformations, as widely observed in experiments and simulations.

DOI: 10.1103/PhysRevLett.127.015501

Identifying the mechanism of plastic deformation in amorphous solids, such as glasses, is one of the major unsolved problems in condensed matter physics. In crystals, plastic flow is mediated by dislocations. These are topological defects corresponding to one missing crystalline plane in the lattice (edge dislocations) or to a lattice plane shifted by one layer (screw dislocations). While the mechanism of dislocation-mediated plastic deformation in crystals was already figured out in seminal work by Taylor [1], Polanyi [2], and Orowan [3] in 1934, a comparable mechanistic understanding of plastic deformation in glasses is still missing.

Numerical simulation studies and earlier theories of plastic activity in glasses have established the existence of so-called shear transformation zones (STZs) [4]. These arise in regions where atomic motions are strongly nonaffine, i.e., with additional (nonaffine) displacements on top of those (affine) dictated by the macroscopic strain, that are required from mechanical equilibrium [5,6]. However, STZs have remained poorly characterized in terms of their structure and topology, until pioneering work by Procaccia and co-workers [7] suggested that STZs can be identified with Eshelby-like quadrupolar events in the displacement field that self-organize into 45° shear bands to minimize the elastic energy [7] (see also [8]). Although this mechanism of self-organization of quadrupoles can explain observations of sinusoidal density fluctuations in shear bands of metallic glasses [9,10], the quadrupoles are not the only shape of plastic instabilities, and in certain systems are rarely observed or not observed at all [11,12].

In this Letter, we provide the more general answer to the problem of identifying the mechanism of plastic instability in amorphous solids and its topological nature. We start by showing that the (nonaffine) displacement field of glasses presents well-defined topological singularities connected with the breakdown of the compatible deformation condition, which we demonstrate here for the first time for glasses. These topological structures are similar to dislocations (and/or vortices in superfluids), with the important difference that dislocations in crystals appear in the undeformed lattice, whereas here they appear in the displacement field under deformation. This is linked to the intrinsic out-of-equilibrium nature of glasses and it is also a fundamental difference with respect to earlier works that aimed at describing dislocations in the static structure of undeformed glass [13–16].

We show that these dislocation-like topological defects (DTDs) are the carriers of plasticity because they lead to an average Burgers vector that strongly correlates with plastic events and displays a strong global peak at the yielding

point. This yielding peak is highly correlated throughout the material, as expected for a sample-spanning slip system. Based on this evidence, a consistent theoretical description of plasticity in amorphous solids can be formulated, with predictions in excellent agreement with observations.

The mechanical deformation in a material can be characterized by the displacement (vector) field u_i [17,18], which defines the deviations of the material points from their original positions (x_i) in the undeformed frame:

$$x_i' = x_i + u_i. \tag{1}$$

The i index here indicates the different spatial directions $i = (x, y, z)$. The displacement vector can be decomposed into its affine and nonaffine contributions [19]:

$$u_i = u_i^A + u_i^{NA} = \Lambda_i^k x_k + u_i^{NA}, \tag{2}$$

where Λ_i^k is a matrix of constants. Nonzero nonaffine displacements u_i^{NA} arise in glasses and noncentrosymmetric crystals in order to preserve mechanical equilibrium in the affine position dictated by the applied strain field [5,6,20]. In ordered crystals, the strain tensor $\epsilon_{ij} \equiv \partial_{(i} u_{j)}$ obeys the so-called compatibility constraint [21,22]:

$$\nabla \times \nabla \times \boldsymbol{\epsilon} = 0, \tag{3}$$

which is equivalent to saying that du_i is a closed differential form.

More in general, considering the total displacement field, one can define a Burgers vector [23] as the line integral of the vector field du_i on a closed loop $\mathcal{L}$,

$$b_i \equiv -\oint_{\mathcal{L}} du_i = -\oint_{\mathcal{L}} \frac{du_i}{dx^k} dx^k. \tag{4}$$

As shown below, the Burgers vector vanishes for affine displacements and it is finite for nonaffine ones:

$$b_i^A = 0, \qquad b_i^{NA} \neq 0. \tag{5}$$

A nonvanishing Burgers vector indicates the presence of topological defects inside the loop $\mathcal{L}$. In particular, it is associated to a nontrivial winding number around the line defect. The presence of a finite Burgers vector is equivalent with the explicit breaking of an emergent topological symmetry expressed in terms of the conservation of a two-form current $J_I^{\mu\nu}$ [24,25]:

$$\partial_\mu J_I^{\mu\nu} \neq 0, \quad \text{with} \quad J_I^{\mu\nu} \equiv \epsilon^{\mu\nu\rho} \partial_\rho u_I, \tag{6}$$

which plays the exact same role of the Bianchi identity in the classical covariant Maxwell formulation of electromagnetism (EM) [26,27]. In other words, the presence of defects and a finite Burgers vector is in 1-to-1 correspondence to the existence of magnetic monopoles in EM [28].

Other typical examples are those of dislocations in crystals and vortices in superfluids [23,29–32]. The role of these generalized global symmetries has been recently recognized to be crucial to classify topological phases of matter á la Landau [33–35]. For more details regarding the connection between generalized global symmetries and nonaffine displacements see the related paper [25].

In [25] we showed more formally that the nonaffine dynamics typical of liquids and amorphous systems necessarily implies the presence of finite Burgers vectors and topological defects. In this Letter, we take one step forward and demonstrate these concepts on glass deformation data taken from numerical simulations of a coarse-grained (flexible-chain) polymer glass well below the glass transition used in previous work [36], undergoing athermal quasistatic (AQS) shear deformation.

In Fig. 1 we show a typical snapshot of the displacement field at strain $\gamma = 0.08$, with a system-spanning Burgers circuit. Several regions with strongly nonaffine configurations exhibiting vortexlike shape are found. At those points, the displacement field is not single valued and the integral of the Burgers vector around those region is nonzero.

The displacement field was measured from the MD simulation and subsequently subjected to an interpolation procedure to obtain a smooth field for further formal calculations (for details see the Supplementary Material [37]). Evaluating the Burgers integral according to Eq. (4) gives a nonzero Burgers vector b_i. As shown in the Supplemental Material [37], the same calculation on a purely affine displacement field gives $b_i = 0$. Then in Eq. (6), this implies that the displacement field is single valued and $\partial_\mu J_I^{\mu\nu} \neq 0$. This also implies the violation of the compatibility condition [38] already in the small deformation (elastic) regime of glasses, which was speculated to occur when the deformation is nonaffine [39], and that we demonstrate here for the first time for glasses. This finding also indicates that not only the reference metric space is curved [16], but also that the affine connections (Christoffel symbols) are not symmetric in their lower indices and the Einstein-Cartan torsion tensor is nonzero [40]. Importantly, while the above facts have been established in crystal plasticity for large plastic deformations [38], we demonstrate here microscopically that they apply to glasses even in the elastic infinitesimal deformation regime, providing a direct link between geometry and plasticity.

To make the analysis of the data robust, 10 replicas were created and each was analyzed with stress-strain and Burgers vector analysis of the DTDs. The results are shown in Fig. 2. As already anticipated, the norm of the Burgers vector $|b_i|$ averaged over the different replicas displays a dominant and sharp peak at the location of the yielding point, around $\gamma \approx 0.1$. As shown explicitly in the Supplemental Material [37], (I) the norm of the Burgers

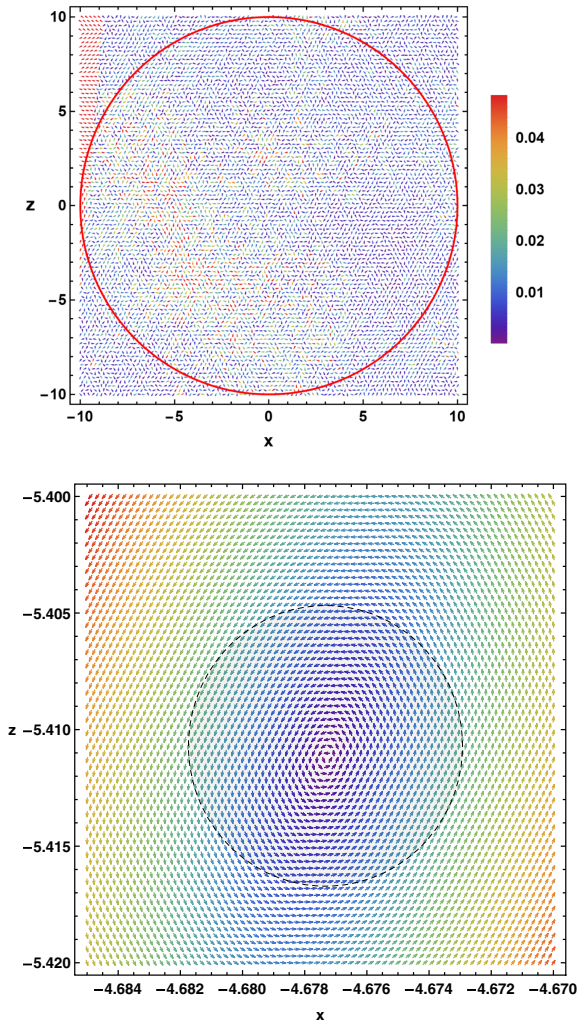

FIG. 1. Top: a snapshot of the interpolated 2D displacement field u_i for a single replica at $\gamma = 0.08$. The colors indicate the amplitude of the displacement field $|\vec{u}|$. The red curve is the closed Burgers loop with $R = 10$ on which the Burgers vector is computed using Eq. (4). Bottom: zoom around a strongly nonaffine region with vortexlike shape.

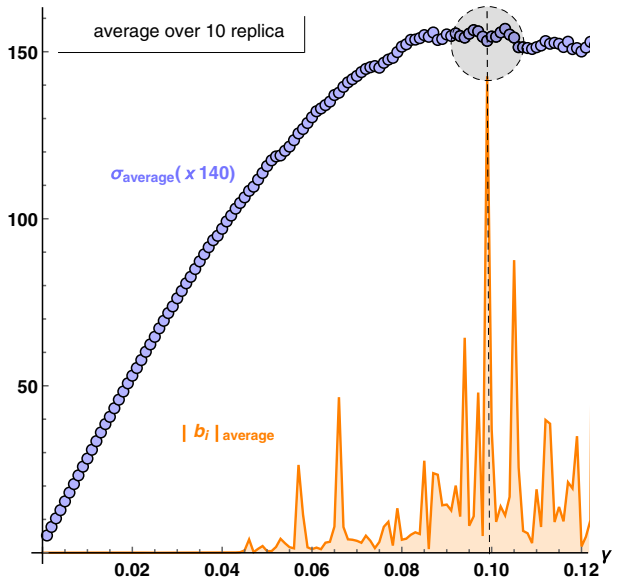

FIG. 2. The magnified stress-strain curve (purple circles) and the norm of the Burgers vector $|b_i|$ (orange) averaged over 10 independent replicas. The vertical dashed line indicates the location of the main peak. The gray shaded area emphasizes the position of the yielding point.

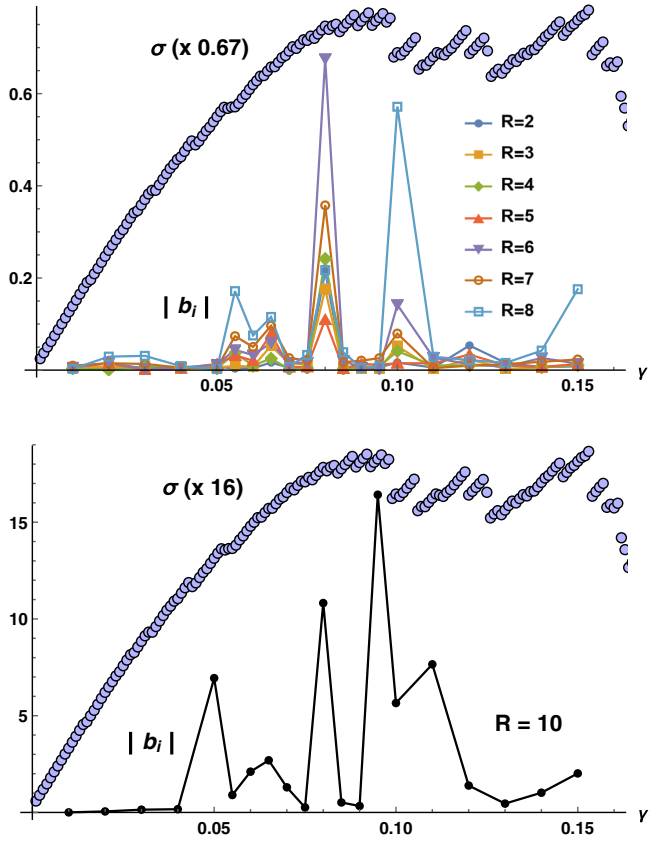

FIG. 3. Top: the norm of the Burgers vector $|b_i|$ as a function of the closed loop radius R for a single replica. The corresponding stress-strain curve is in purple. Bottom: the same plot with the norm of the Burgers vector for $R = 10$.

vector computed on the single replica is able to locate not only the yielding point but also the secondary plastic events manifest in the stress-strain curve as sudden stress falloff. Strikingly, we observe clear peaks of $|b_i|$ in correspondence of these mechanical instabilities signaled by nearly zero or slightly negative eigenvalues of the Hessian matrix [41,42]. In addition, (II) the norm of the Burgers vector is independent of the topology of the closed Burgers loop. This is a manifestation of the topological nature of this object, which "counts" the nonaffine displacements inside the close loop and demonstrates that these DTDs are genuine topological invariants.

In Fig. 3 we present a different analysis of the same data, where now we vary the linear size of the Burgers circuit used to measure the norm $|b_i|$ as a function of strain. This analysis reveals much of the spatial extent of the various

plastic events. It is seen that, on increasing the linear size of the Burgers circuit $\mathcal{L}$ or its radius R, the peak of $b_i|$ corresponding to the yield point $\gamma = 0.1$, grows enormously, much more than the peaks of the plastic events at $\gamma = 0.05$–0.06 and $\gamma = 0.08$, and even more than the post-yielding peaks at $\gamma = 0.15$. This fact indicates the formation of a slip system spanning the whole material right at yielding, consistent with the formation of shear bands in Fig. 4. A systematic plot of the Burgers peak amplitudes as a function of loop radius R for plastic events at varying γ is shown in the Supplemental Material [37].

Based on the above observations, it is possible to formulate a mechanism of strain softening and plastic yield in glasses mediated by DTDs and their mutual interaction. After having verified Eq. (4) on the basis of the MD simulations, and assuming polar coordinates (z, θ), the displacement field around a DTD follows immediately as $u_i = b_i\theta/2\pi$, with the corresponding local elastic strain field being singular, $\epsilon_{\theta z} = \epsilon_{z\theta} = b/4\pi r$ [43], where $b \equiv |b_i|$ is the modulus of the Burgers vector.

By simple geometry [25], one can show that $|b_i| \propto |u_i^{NA}|$. In turn, from theory, numerical simulations, and experiments [19,44–46], it is known that $|u_i^{NA}| \propto \gamma$, where $|u_i^{NA}|$ is an average over the sample. This implies that, due to the nature of nonaffine displacements to grow with γ, $|b_i|$ has, on average, a tendency to grow with the applied strain γ as well. This is not exactly what emerges from the single replica shown in the Supplemental Material [37], where the behavior of $|b_i|$ vs γ is rather noisy and intermittent and occurs mainly through bursts (peaks) in correspondence of major plastic events, and it is these bursts that grow as γ increases. Although a precise mechanism for DTD multiplication and growth on increasing the strain is yet to be identified, it becomes statistically more likely that DTDs begin to interact with each other in the plastic events where $|b_i|$ becomes large. In particular, there is an increased likelihood that two DTDs come together with antiparallel Burgers vectors b_1 and b_2. It can be shown, using the Peach-Köhler force, that this gives rise to an attractive interaction force given by [18]

$$f = -\frac{Gb_1b_2}{2\pi r}, \tag{7}$$

where b_1 and b_2 are the moduli of the Burgers vectors of the two interacting DTDs and G is the shear modulus. This force is clearly large around the main plastic events where $|b|$ is large.

Hence, it is possible to have a mechanism whereby the rate of encounter and "coagulation" between two DTDs with antiparallel Burgers vector becomes large. DTDs therefore attract each other, with an effective attraction force given by Eq. (7), and tend to coagulate into larger aggregates in correspondence of plastic events. This shear-induced aggregation process eventually leads to the formation of slip systems (i.e., shear bands), as the strain increases.

By leveraging these concepts, it is also possible to predict the orientation of the slip systems. Let $\sigma = F/A_0$ be the tensile stress acting on the sample, e.g., a uniaxial stress, with F the applied tensile force and A_0 the sample cross section area. Denoting with ϕ the angle between the normal to the slip plane and the direction of the tensile force F, and with λ the angle between the slip direction and the direction of F, the slip plane area is thus given by $A_s = A_0/\cos\phi$. Hence the tensile force resolved in the slip direction, $F\cos\lambda$, gives rise to a resolved shear stress given by the well-known Schmid's law [47,48]:

$$\sigma_{RSS} = \sigma\cos\phi\cos\lambda. \tag{8}$$

In general, the three directions are not coplanar; hence $\phi + \lambda \neq 90°$, while $\phi + \lambda = 90°$ is the minimum possible value [47,48]. DTDs will, in general, aggregate into slip bands that are oriented randomly. For a given σ, slip systems will therefore be initiated by facilitated motion of DTDs that self-organize in a slip plane that experiences the largest resolved shear stress σ_{RSS}, similar to what happens with avalanches that initiate in a spatial direction where the resolved stress is largest and thus can overwhelm frictional resisting forces. The largest resolved stress clearly corresponds to the maximum value of $\cos\phi\cos\lambda$. Under the constraint $\min(\phi + \lambda) = 90°$, this happens for $\phi = \lambda = 45°$. Hence, for a uniaxial deformation or for a simple shear deformation, shear bands due to aggregation of DTDs will form at an angle of 45° with respect to the tensile axis as observed in our MD simulations (Fig. 4), as well as other simulations and experiments [7,9,10].

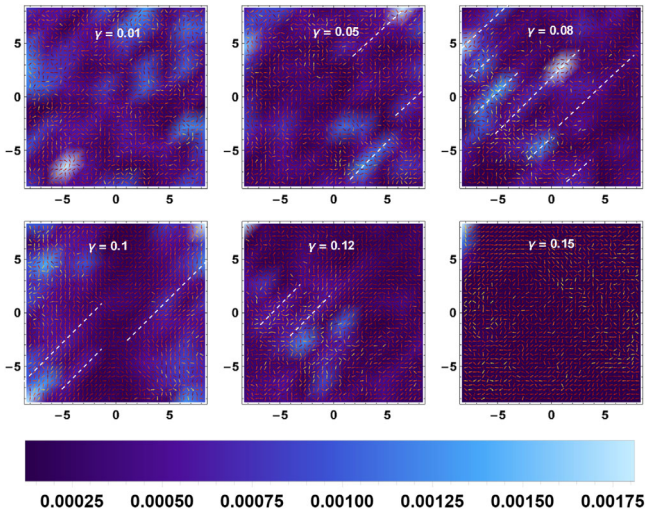

FIG. 4. The evolution of the displacements vector $\vec{u}$ by increasing the external strain γ. The background color shows the Burgers vector norm and the arrow its direction and local amplitudes. The dashed white lines guide the eye toward the 45° shear band forming.

In summary, we have shown that nonaffine displacements in the deformation of amorphous materials lead all the way to the formation of topological singularities (DTDs) in the displacement field, which can be quantitatively characterized by Burgers vectors. We have demonstrated that DTDs are responsible for plastic events on the example of athermal quasistatic shear of model polymer glasses quenched at low temperature. The spatially averaged norm of the Burgers vectors displays peaks corresponding to the plastic events, and an extremely evident nonlocal (system-spanning) peak at the yield point. Treating DTDs in analogy to dislocations may allow one to formulate a self-consistent mechanism of slip band formation due to the attractive force between antiparallel DTDs and to their growing population on increasing the strain. The preferential alignment of coagulated DTDs (shear bands) along the 45° direction with respect to the tensile axis is predicted by Schmid's law, in agreement with all experiments and numerical simulations. This work provides the quantitative identification of the long-sought "defects" that mediate fluidity and plasticity in amorphous solids [49]. Different from crystals, and from earlier work on glasses [13], the dislocationlike topological defects are not to be found in the static structure but, crucially, in the displacement field under deformation. Furthermore, they originate directly from nonaffine displacements [5,6,19]. Because the nonaffine displacements in turn originate from the locally low degree of centrosymmetry in the static structure of amorphous systems, which is quantifiable [50,51], this finding opens up the way for identifying the structural signatures of plasticity in glasses [52–54], but now in terms of atomistically well-defined quantities. Furthermore, it can provide a metric to better distinguish ductile from brittle first order–like failure [52,55].

Finally, this work provides a quantitative identification of topological effects in amorphous systems [56], leading to a new geometrical description of plasticity and deformations in glasses. This has potential to open new directions in the chase for "order" in disordered systems.

We thank Michael Landry for discussions and collaboration on related ideas and Giorgio Torrieri, Zohar Nussinov and Yun-Jiang Wang for fruitful discussions and helpful comments. M. B. acknowledges the support of the Shanghai Municipal Science and Technology Major Project (Grant No. 2019SHZDZX01). A. Z. and I. K. acknowledge financial support from U.S. Army Research Laboratory and U.S. Army Research Office through Contract No. W911NF-19-2-0055.

*Corresponding author.
alessio.zaccone@unimi.it
†b.matteo@sjtu.edu.cn
‡kruchevskyivan@gmail.com
§timothy.w.sirk.civ@mail.mil

[1] G. I. Taylor, Proc. R. Soc. Ser. A **145**, 362 (1934).
[2] M. Polanyi, Z. Phys. **89**, 660 (1934).
[3] E. Orowan, Z. Phys. **89**, 605 (1934).
[4] M. L. Falk and J. S. Langer, Phys. Rev. E **57**, 7192 (1998).
[5] A. Lemaître and C. Maloney, J. Stat. Phys. **123**, 415 (2006).
[6] A. Zaccone and E. Scossa-Romano, Phys. Rev. B **83**, 184205 (2011).
[7] R. Dasgupta, H. G. E. Hentschel, and I. Procaccia, Phys. Rev. Lett. **109**, 255502 (2012).
[8] E. De Giuli, Phys. Rev. E **101**, 043002 (2020).
[9] V. Hieronymus-Schmidt, H. Rösner, G. Wilde, and A. Zaccone, Phys. Rev. B **95**, 134111 (2017).
[10] D. Şopu, A. Stukowski, M. Stoica, and S. Scudino, Phys. Rev. Lett. **119**, 195503 (2017).
[11] X. Cao, A. Nicolas, D. Trimcev, and A. Rosso, Soft Matter **14**, 3640 (2018).
[12] A. Ghosh, Z. Budrikis, V. Chikkadi, A. L. Sellerio, S. Zapperi, and P. Schall, Phys. Rev. Lett. **118**, 148001 (2017).
[13] P. Chaudhari, A. Levi, and P. Steinhardt, Phys. Rev. Lett. **43**, 1517 (1979).
[14] P. J. Steinhardt and P. Chaudhari, Philos. Mag. A **44**, 1375 (1981).
[15] A. Acharya and M. Widom, J. Mech. Phys. Solids **104**, 1 (2017).
[16] M. Moshe, I. Levin, H. Aharoni, R. Kupferman, and E. Sharon, Proc. Natl. Acad. Sci. U.S.A. **112**, 10873 (2015).
[17] P. Chaikin and T. Lubensky, *Principles of Condensed Matter Physics* (Cambridge University Press, Cambridge, England, 2000).
[18] L. Landau and E. Lifshitz, *Theory of Elasticity: Volume 6* (Pergamon Press, New York, 1986).
[19] B. A. DiDonna and T. C. Lubensky, Phys. Rev. E **72**, 066619 (2005).
[20] B. Cui, A. Zaccone, and D. Rodney, J. Chem. Phys. **151**, 224509 (2019).
[21] A. E. H. Love, *A Treatise on the Mathematical Theory of Elasticity* (Cambridge University Press, Cambridge, England, 1892).
[22] E. Beltrami, *Sull'interpretazione Meccanica Delle Formole di Maxwell: Memoria* (Tipografia Gamberini e Parmeggiani, Bologna, 1886).
[23] H. Kleinert, *Gauge Fields in Condensed Matter*, Gauge Fields in Condensed Matter No. Vol. 2 (World Scientific, Singapore, 1989).
[24] S. Grozdanov and N. Poovuttikul, J. High Energy Phys. 04 (2019) 141.
[25] M. Baggioli, M. Landry, and A. Zaccone, arXiv:2101.05015.
[26] J. Zaanen, Z. Nussinov, and S. Mukhin, Ann. Phys. (Amsterdam) **310**, 181 (2004).
[27] S. Grozdanov, D. M. Hofman, and N. Iqbal, Phys. Rev. D **95**, 096003 (2017).
[28] S. Grozdanov and N. Poovuttikul, Phys. Rev. D **97**, 106005 (2018).
[29] A. J. Beekman, J. Nissinen, K. Wu, K. Liu, R.-J. Slager, Z. Nussinov, V. Cvetkovic, and J. Zaanen, Phys. Rep. **683**, 1 (2017), dual gauge field theory of quantum liquid crystals in two dimensions.
[30] V. Cvetkovic, Z. Nussinov, and J. Zaanen, Philos. Mag. **86**, 2995 (2006).

[31] V. Cvetkovic, Z. Nussinov, and J. Zaanen, arXiv:0905.2996.
[32] P. Ronhovde, S. Chakrabarty, D. Hu, M. Sahu, K. K. Sahu, K. F. Kelton, N. A. Mauro, and Z. Nussinov, Eur. Phys. J. E **34**, 105 (2011).
[33] A. Kapustin and R. Thorngren, arXiv:1309.4721.
[34] D. Gaiotto, A. Kapustin, N. Seiberg, and B. Willett, J. High Energy Phys. 02 (2015) 172.
[35] B. Yoshida, Phys. Rev. B **93**, 155131 (2016).
[36] V. V. Palyulin, C. Ness, R. Milkus, R. M. Elder, T. W. Sirk, and A. Zaccone, Soft Matter **14**, 8475 (2018).
[37] See Supplemental Material at http://link.aps.org/supplemental/10.1103/PhysRevLett.127.015501 for details of the numerical simulations and analytical reconstruction of the microscopic deformation field.
[38] A. Acharya and J. Bassani, J. Mech. Phys. Solids **48**, 1565 (2000).
[39] J. A. Zimmerman, D. J. Bammann, and H. Gao, Int. J. Solids Struct. **46**, 238 (2009).
[40] M. L. Ruggiero and A. Tartaglia, Am. J. Phys. **71**, 1303 (2003).
[41] L. Gartner and E. Lerner, Phys. Rev. E **93**, 011001(R) (2016).
[42] J. Yang, J. Duan, Y. J. Wang, and M. Q. Jiang, Eur. Phys. J. E **43**, 56 (2020).
[43] M. Kleman and O. D. Lavrentovich, *Soft Matter Physics: An Introduction* (Springer, New York, 2003).
[44] A. Zaccone, Mod. Phys. Lett. B **27**, 1330002 (2013).
[45] M. Laurati, P. Maßhoff, K. J. Mutch, S. U. Egelhaaf, and A. Zaccone, Phys. Rev. Lett. **118**, 018002 (2017).
[46] K. L. Galloway, D. J. Jerolmack, and P. E. Arratia, Soft Matter **16**, 4373 (2020).
[47] E. Schmid and W. Boas, Theorien der kristallplastizität und -festigkeit, in *Kristallplastizität: Mit Besonderer Berücksichtigung der Metalle* (Springer Berlin Heidelberg, Berlin, Heidelberg, 1935), pp. 279–301.
[48] T. H. Courtney, *Mechanical Behavior of Materials* (Waveland Press, Long Grove, IL, 2005).
[49] R. Benzi, M. Sbragaglia, M. Bernaschi, S. Succi, and F. Toschi, Soft Matter **12**, 514 (2016).
[50] R. Milkus and A. Zaccone, Phys. Rev. B **93**, 094204 (2016).
[51] C. L. Kelchner, S. J. Plimpton, and J. C. Hamilton, Phys. Rev. B **58**, 11085 (1998).
[52] D. V. Denisov, M. T. Dang, B. Struth, A. Zaccone, G. H. Wegdam, and P. Schall, Sci. Rep. **5**, 14359 (2015).
[53] E. D. Cubuk, R. J. S. Ivancic, S. S. Schoenholz, D. J. Strickland, A. Basu, Z. S. Davidson, J. Fontaine, J. L. Hor, Y.-R. Huang, Y. Jiang, N. C. Keim, K. D. Koshigan, J. A. Lefever, T. Liu, X.-G. Ma, D. J. Magagnosc, E. Morrow, C. P. Ortiz, J. M. Rieser, A. Shavit *et al.*, Science **358**, 1033 (2017).
[54] D. Richard, M. Ozawa, S. Patinet, E. Stanifer, B. Shang, S. A. Ridout, B. Xu, G. Zhang, P. K. Morse, J.-L. Barrat, L. Berthier, M. L. Falk, P. Guan, A. J. Liu, K. Martens, S. Sastry, D. Vandembroucq, E. Lerner, and M. L. Manning, Phys. Rev. Mater. **4**, 113609 (2020).
[55] M. Ozawa, L. Berthier, G. Biroli, A. Rosso, and G. Tarjus, Proc. Natl. Acad. Sci. U.S.A. **115**, 6656 (2018).
[56] A. G. Grushin, arXiv:2010.02851.